

Article

Automatic EMI Filter Design for Power Electronic Converters Oriented to High Power Density

Graziella Giglia ^{1,*} , Guido Ala ¹, Maria Carmela Di Piazza ² ,
Giuseppe Costantino Giaconia ¹ , Massimiliano Luna ² , Gianpaolo Vitale ²  and
Pericle Zanchetta ³

¹ Dipartimento di Energia, Ingegneria dell'Informazione e Modelli Matematici, Università degli Studi di Palermo, Viale delle Scienze, 90128 Palermo, Italy; guido.ala@unipa.it (G.A.); costantino.giaconia@unipa.it (G.C.G.)

² Istituto di Studi sui Sistemi Intelligenti per l'Automazione, Consiglio Nazionale Delle Ricerche, via Dante 12, 90141 Palermo, Italy; dipiazza@pa.issia.cnr.it (M.C.D.P.); luna@pa.issia.cnr.it (M.L.); vitale@pa.issia.cnr.it (G.V.)

³ Department of Electrical and Electronic Engineering, University of Nottingham, University Park, Nottingham NG7 2RD, UK; Pericle.Zanchetta@nottingham.ac.uk

* Correspondence: graziella.giglia@unipa.it

Received: 18 December 2017; Accepted: 16 January 2018; Published: 18 January 2018

Abstract: In this paper, a complete computer aided procedure based on the power density concept and aimed at the automatic design of EMI filters for power electronic converters is presented. It is rule-based, and it uses suitable databases built-up by considering information on passive components available from commercial datasheets. The power density constraint is taken into consideration by imposing the minimization of the filter volume and/or weight; nevertheless, the system in which the automatically designed filter is included satisfies the electromagnetic compatibility standards limits. Experimental validations of the proposed procedure are presented for two real case studies, for which the performance and the size of the best filter design are compared with those related to a conventionally designed one.

Keywords: EMI filter; power converter; power density; optimal design; electrical drives

1. Introduction

The use of power electronic converters is very common in many industrial applications such as in the aeronautic and automotive fields, in hybrid vehicles, and in the electric aircraft context. This trend usually generates a reduction of the installation cost, but low volume and weight requirements are very important to facilitate installation, handling, and maintenance operations of the power converter. High power density power electronic converters are becoming increasingly essential for future markets [1,2].

The use of power devices with high speed commutation makes such systems unintentional EMI sources. Therefore, EMI attenuation solutions are necessary to ensure both the reliability and the electromagnetic compatibility of the system of which the power electronic converter is a part. In particular, EMI filtering is required to ensure the compliance with the emission limits imposed by the stringent technical standards [3–12], and behavioral models of electric motors can also be used to predict conducted interferences [13]. It is worth noting that electromagnetic compatibility and power density in power electronic converters are closely related issues.

The EMI filter is a part of the power electronic converter and it can significantly influence its size and weight. In order to address this issue, besides satisfying EMI limits, a further reduction of the filter size/weight is a requirement of crucial importance in the design phase [1,14,15].

The power density feature of EMI filters has been treated in scientific literature, but the presented techniques cannot be applied in a general way. In fact, some of these techniques propose only the use of high-performance magnetic materials to reduce the inductor core's size [15]. In [16], some aspects for the design of high-density EMI filters for DC-fed motor drives are discussed and, in particular, grounding issues, circuit topologies, and some strategies to reduce the overall filter size are covered. In [17], the impedance interaction between the EMI filter and the noise propagation path, and its influence on the common mode (CM) filter design, are investigated; by applying this method, the impedance-mismatching concept is used to obtain a reduction of the CM inductor value that can potentially achieve a high power density. However, this method is only applied to a CM EMI filter design.

Other approaches propose the use of genetic algorithms to perform an EMI filter design [18]. In those cases, optimal solutions are usually obtained with a great number of iterations, thus resulting in a time consuming task.

In [19], the authors present software for designing EMI filters, limited only to one filter topology; the authors do not include the possibility of a discrete differential mode (DM) choke selection. Moreover, the paper only provides data about the CM core size, and the choice is not based on optimization.

In [20,21], a minimization of the filter volume is performed by using interpolated volumetric parameters. This approach can only be applied to the DM filter components and not to CM components because a parametrization of the volume curves is not possible for most of the commercially available CM chokes. Finally, a systematic approach for the volume optimization of a two-stage DM and CM EMI filter, essentially based on the ratio between the CM and DM inductance of the first filter stage, is proposed in [22].

After having defined both the EMI filter topology and the component values, the EMI filter can be setup according to a considerable number of feasible configurations. The conventional design of EMI filters, based on a trial and error approach, requires significant effort in terms of time, and it does not guarantee the optimal choice of filter components to obtain the maximum power density.

The first results of a rule-based computer-aided general procedure for the optimal design of EMI filters in terms of volume minimization have been proposed in [23] by the same authors.

In this paper, a comprehensive automatic procedure has been set-up; the procedure allows the design of the best filter configuration in a simple and fast way. Power density impact evaluation (i.e., volume, weight) of the filter configuration has been carried out, thus achieving useful results for engineers and scientists. The proposed algorithm can be implemented using any software programming environment and has a low computational demand.

Furthermore, suboptimal configurations can be compared with each other and with the best one so as to allow the designer to make the final choice and to also match further commercial constraints, if there are any.

The proposed procedure starts from the basic principle of conventional EMI filter design and considers the additional objective of pursuing the best power density for the EMI filter. A suitable test set-up enables one to obtain an experimental assessment of the automatic design procedure by comparing volume, weight, and performance.

2. The Rule-Based Computer-Aided EMI Filter Design Procedure

A multistage EMI filter configuration usually provides a stronger filter attenuation; consequently, it determines a higher cutoff frequency value than that obtained with a single stage filter. Furthermore, a higher value of the cutoff frequency leads to smaller values of the filter components and to physically smaller components. Therefore, even if the number of passive components is larger in a multistage configuration, overall, the latter may exhibit a smaller volume/weight than a single stage filter as has been demonstrated for the DM mode in [20]. However, it depends on the CM and DM required attenuations, on the electrical characteristics of the power electronic circuit under study, and on the

adopted filter components. A verification of all feasible configurations is necessary to assess which of them allows one to obtain the best power density; the achievement of a trade-off is not a trivial task due to the broad variety of components that the market offers. Therefore, the choice of the best filter design, in terms of maximization of the power density, is not ensured by following a conventional design procedure.

The proposed design procedure is a rule-based algorithm that takes into account the characteristics of the filter application: the power electronic circuits, the constraints of the filter design, and the databases of commercial components for the setup of the EMI filters. The flowchart of the design method is shown in Figure 1, in which AWG is the conducting wire diameter; n_{stages} is the number of filter stages; N_{max} is the maximum number of turns for each core; C_y and C_x define the capacitance of phase-to-ground and phase-to-phase capacitors, respectively; V_{C_rated} and C_{rated} indicate the capacitor rated voltage/capacitance, respectively; V_N is the rated voltage of the power converter; and B_{max} and B_{sat} are the maximum/saturation magnetic induction values, respectively.

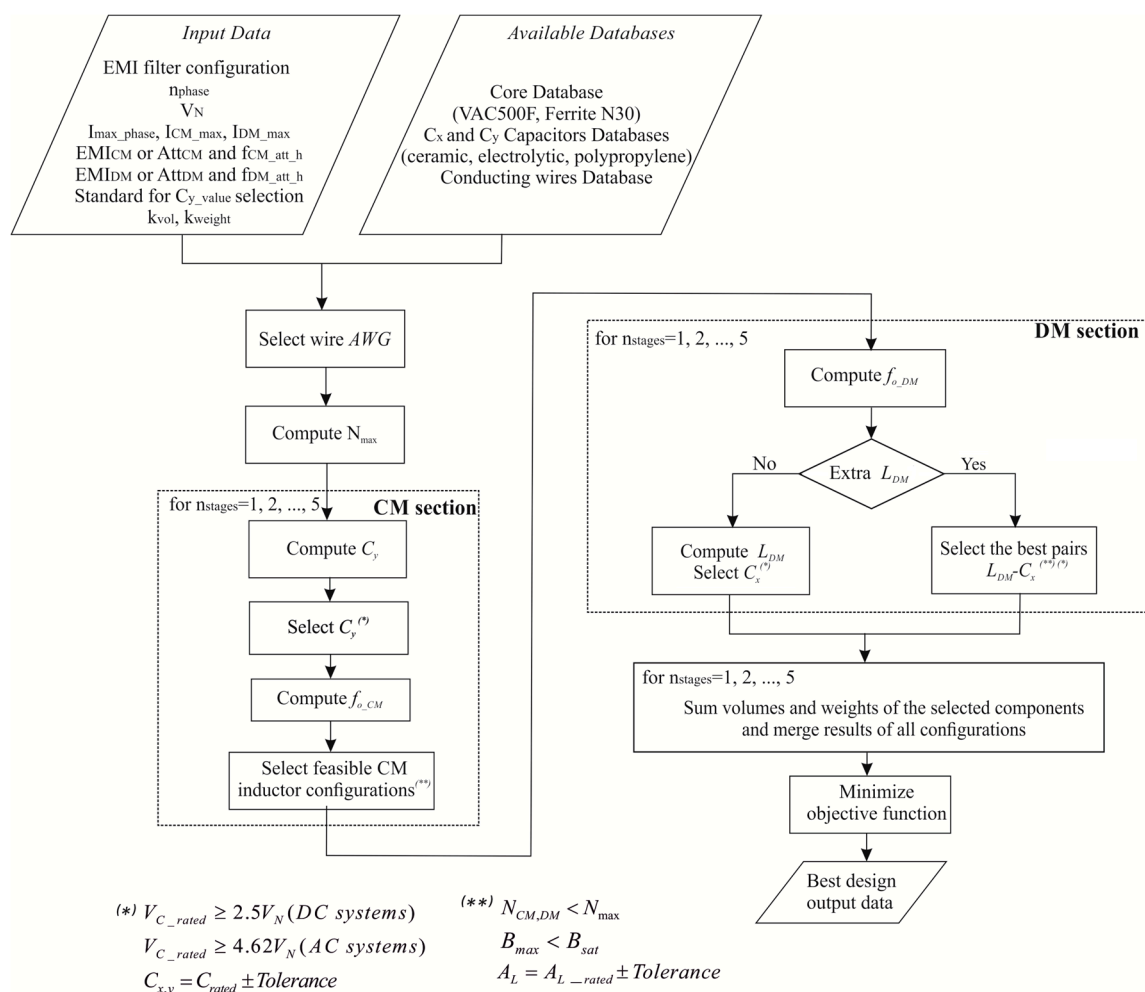


Figure 1. Flowchart of the proposed design method.

Firstly, the designer must define the following *Input Data*:

- EMI filter topology (e.g., Γ , Π , T);
- n_{phase} : number of AC phases or DC lines of the power electronic system;
- V_N : rated voltage of the power converter;
- I_{max_phase} : maximum operating current;

- I_{CM_max} , I_{DM_max} : maximum value of the CM and DM currents;
- *Standard for C_y value selection*: the CM capacitance value limits the ground current and thus it is related to safety issues. Either the SAE AES 1831 standard or the maximum ground leakage current are taken into consideration to define the capacitance value;
- k_{vol} , k_{weight} : coefficients provided by the designer which allow one to obtain the best design, assuming any linear combination of volume and weight as the objective function;
- filter design can be performed either on the basis of the measured CM/DM spectra (EMI_{CM} , EMI_{DM}), or by explicitly giving the required CM/DM attenuations (Att_{CM} , Att_{DM}) and the CM/DM component frequencies to be attenuated ($f_{CM_att_h}$ and $f_{DM_att_h}$). In the first case, the algorithm identifies the crucial point among the more relevant peaks at the lowest frequencies on the EMI spectra. Then, it computes the required attenuations for the CM and DM noise as expressed in (1) and (2), respectively:

$$Att_{CM} = A_{h_CM} - A_{max} + \Delta \quad (1)$$

$$Att_{DM} = A_{h_DM} - A_{max} + \Delta \quad (2)$$

where A_{h_CM} and A_{h_DM} are the amplitudes of the frequency spectrum components to be attenuated; A_{max} is the maximum amplitude allowed by the standard; and Δ is a safety margin (usually 6 dB μ V).

For the reader's convenience, it is worth recalling that EMI filters are generally low-pass passive filters realized with inductors and capacitors. The adopted arrangements can be Γ , Π , and T with longitudinal inductors and transversal capacitors. The choice of the passive filter topology is related both to the theoretical attenuation value of the chosen filter configuration (i.e., 40 dB/dec for Γ type L-C single stage, 60 dB/dec for Π or T type L-C single stage, etc.) and to the equivalent impedance magnitude of the equipment under test (EUT) and of the noise receiver. Therefore, a preliminary step for a proper EMI filter design is to suitably choose the filter topology by taking into account the criterion of maximum impedance mismatching between the source and the receiver.

Three databases of devices available on the market have been set up. The first one includes magnetic cores and it is populated with the following relevant data:

- core material and model;
- geometric dimensions and weight;
- inductance factor A_L (μ H/1 turn) at 10 kHz and the value of flux density saturation;
- A_L tolerance.

The cores database currently contains components that allow an EMI filter design for applications up to some kW.

Furthermore, a second database of Y-type (CM noise reduction) and X-type (DM noise reduction) capacitors has been created. Ceramic Y-type capacitors, and aluminum electrolytic and polypropylene X-type capacitors for applications with high frequency ripple currents have been included. In particular, the aluminum electrolytic capacitors have a rated voltage of 160 V, 250 V, and 400 V, and a nominal capacitance range of 10 μ F to 330 μ F, whereas the polypropylene capacitors have a minimum rated voltage of 560 V_{DC}/275 V_{AC} (a lower rated voltage for this specific capacitor is not commercially available) and a nominal capacitance range of 0.01 μ F to 10 μ F.

The commercial capacitors database is populated with the following relevant data:

- brand, material, series, model, and package;
- rated capacitance and voltage;
- capacitance tolerance;
- geometric dimensions and weight.

Finally, a third database, including conducting wires, is provided. Hence, the volume/weight contribution given by the inductor wires (which may be relevant when dealing with rated power of

hundreds of Watts and beyond) is included in the EMI filter calculations, and more effective results can be obtained.

After having defined the input data, the conventional design procedure steps are automatically repeated for different arrangements and finally the one which exhibits the best power density is selected.

It has to be underlined that a multi-stage filter may occupy a reduced volume in comparison with a single stage one, as stated in [20]; therefore, the rule-based algorithm analyses all feasible EMI filter designs considering a number of filter stages (n_{stages}) up to five. The evaluation of a maximum number of five stages has been considered by the authors as a reasonable choice.

As shown in Figure 1, the first operation phase is the selection of wire size (AWG) on the basis of the maximum operating current entered by the designer. Then, the maximum number of achievable turns (N_{max}) on each toroidal core of the database is computed as:

$$N_{max} = \frac{2\sigma_{winding}}{360^\circ} \frac{I.C.}{D_{wire}} \tag{3}$$

where $I.C. = \pi(ID_{core} - D_{wire})$ is the inner circumference of the toroidal core, ID_{core} is the inner diameter of the toroidal core, D_{wire} is the wire diameter, and $\sigma_{winding}$ represents the maximum angle that the winding subtends on half of the core. It is acceptable to assume that $\sigma_{winding}$ is equal to 145° (Figure 2).

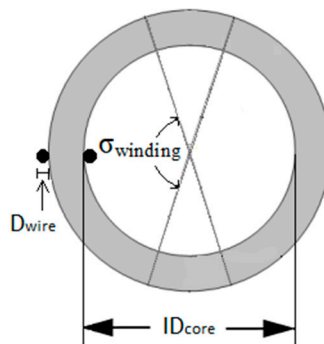


Figure 2. Toroidal core: geometric parameters for Equation (3).

Then, the procedure performs the CM and DM filter design as described below.

2.1. CM Section Design

The procedure calculates, for $n_{stages} = 1, \dots, 5$, the CM capacitance (C_{CM}) and the CM inductance (L_{CM}) as follows:

$$L_{CM} = \frac{1}{C_{CM}(2\pi f_{o_CM})^2} \tag{4}$$

$$C_{CM} = n_{phase} C_y \tag{5}$$

The cutoff or corner frequency ($f_{o_CM/DM}$) is evaluated by considering that the attenuation of an L-C filter starts at this frequency and is rising with $Att_{intr_{CM/DM_filter}}$, which is the inherent filter attenuation strictly related to its topology (e.g., 40 dB/dec for Γ type L-C single stage, 60 dB/dec for Π or T type L-C single stage, etc.). Thus, the required corner frequency can be evaluated according to:

$$Att_{CM/DM} = n_{stages} \times Att_{intr_{CM/DM_filter}} \log \left(\frac{f_{CM/DM_att_h}}{f_{o_CM/DM}} \right) \tag{6}$$

thus obtaining:

$$f_{o_CM/DM} = \frac{f_{CM/DM_att_h}}{10^{\left(\frac{Att_{CM/DM}}{n_{stages} \cdot Att_{infr_{CM/DM_filter}}}\right)}} \quad (7)$$

As already underlined, the more relevant peaks of the EMI spectra are identified together with the corresponding frequencies. Then, for each of these frequencies, the required attenuations are evaluated for the CM and DM noise as expressed in (1) and (2), respectively. The corner frequency is then evaluated by (7) for each of the previous relevant frequencies and among them, the lowest frequency is selected as the cut-off frequency of the L-C filter; this frequency is usually lower than 150 kHz.

Then, the number of turns (N_{CM}) needed to set up the required inductance is computed by (8):

$$N_{CM} = n_{phase} \sqrt{\frac{L_{1_CM}}{A_L}} \quad (8)$$

where $L_{1_CM} = n_{phase} L_{CM}$ is the inductance value of the single CM choke winding. Equation (8) (and also (9) in the following) is derived by considering that for a highly symmetric magnetic core such as the toroidal inductor, the Ampere-law enables one to express the inductance as follows: $L = N^2 A_L$, where A_L is the inverse of the core reluctance evaluated along the centerline of the core l : $A_L = \frac{\mu A}{l}$, A is the cross section area of the core, and μ is the magnetic permeability. Then, the minimum volume C_y capacitor is chosen from the database according to the design constraint $V_{C_y_rated} \geq k \times V_N$, where k is a multiplier factor (equal to 2.5 for DC systems and 4.2 for AC systems [24]). In accordance with the computed value for the CM inductance, the cores allowing the effective realization of the CM choke (i.e., $N_{CM} < N_{max}$) are selected from the database, also verifying the absence of cores saturation.

2.2. DM Section Design

It is possible to choose two alternative procedures by taking into consideration either the leakage inductance of the CM choke (*No extra L_{DM}*) or a DM inductor (*Extra L_{DM}*). The selection between the “No extra L_{DM} ” and “Extra L_{DM} ” procedures is performed by the designer. Moreover, both the procedures can be performed sequentially and then the most appropriate in terms of volume/weight can be selected.

Both procedures include the evaluation of the corner frequency versus the number of stages. Then:

- the “No extra L_{DM} ” procedure computes, for $n_{stages} = 1, \dots, 5$, the leakage inductance of the feasible CM chokes and the corresponding computed value for the DM capacitance.

After the computation of the C_{DM} capacitance, the algorithm selects the capacitor with the minimum volume, according to the design constraint $V_{C_x_rated} \geq k \times V_N$

- in the “Extra L_{DM} ” procedure, for $n_{stages} = 1, \dots, 5$, the DM inductance candidate values are obtained on the basis of the X-capacitors values (ranging between 10 nF and 330 μ F). For each DM core, the number of turns is then computed as follows:

$$N_{DM} = \sqrt{\frac{L_{1_DM}}{A_L}} \quad (9)$$

where $L_{1_DM} = L_{DM}/2$ is the inductance value for each DM core. The cores permitting an effective realization are extracted from the database, in accordance with the $N_{DM} < N_{max}$ constraint and ensuring no saturation. Finally, the feasible L_{DM} - C_x pairs that permit one to setup the DM section according to the design constraints $V_{C_x_rated} \geq k \times V_N$, are selected.

The “Extra L_{DM} ” may be more appropriate when the use of a higher L_{DM} value is preferred to diminish the value or the size of DM capacitors.

The verification of the absence of the CM/DM cores saturation ($B_{max} < B_{sat}$), performed in the design of both sections, allows one to obtain no degradation of the noise mitigation capability of the designed filter configurations.

The procedure also takes into account the component tolerances; in fact, neglecting the tolerances could degrade the filter performance. The capacitors database contains components with a tolerance range of $\pm 20\%$; the cores database contains components with a tolerance of the A_L value from -25% to $+45\%$ and from -30% to $+30\%$ for the vitroperm and ferrite materials, respectively. The negative tolerance percentage determines a degradation of the filter performance because it implies an actual value of the component lower than the nominal one and consequently a cutoff frequency higher than that required; hence, the filter will begin to attenuate at a higher frequency than the desired one. This issue is taken into account by choosing the commercial components based on the value related to the negative tolerance.

Finally, the EMI filter volume and weight of all realizable arrangements are computed and the one with the best power density is selected. A comparison among suboptimal results and the best arrangement is also allowed.

The filter configurations obtained by the automatic procedure are related to the specific components included in the databases, whose number and typology can be increased, if needed.

3. Experimental Setup

The automatic design procedure has been validated by experimental investigations by using a suitably devised test bench.

A PWM IGBT Voltage Source Inverter (VSI) supplying a three-phase load has been considered. The inverter is setup by a STGIPS10K60A power module and an Altera Cyclone III FPGA board realizing the PWM.

The inverter switching frequency is set to 20 kHz and the output voltage is 48 V.

A DC Line Impedance Stabilization Network (LISN) is used, with a voltage potentiality up to 600 V [25].

In order to assess the validity of the proposed approach, two case studies are considered with different three-phase loads:

- Case study #1: a 220 W induction motor, commonly used both in vehicles (road and marine vehicles, aircraft) and in DC systems, such as those installed in some residential/commercial smart buildings [26,27];
- Case study #2: a symmetric resistive load with low-power (7.2 W).

The experimental configuration scheme is given in Figure 3.

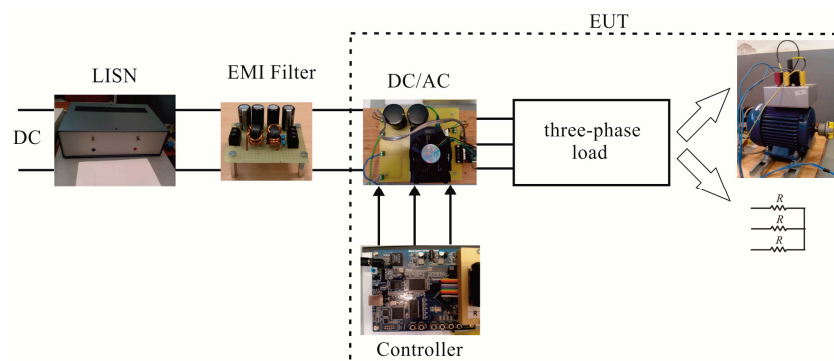


Figure 3. Block diagram of the experimental rig.

4. Experimental Validation and Discussion

Experimental measurements and plate values are the inputs required for the proposed computer-aided design methodology.

The EMI measurements have been carried out by using an RF current probe R&S EZ-17 (20 Hz–100 MHz, maximum DC current equal to 300 A) and an R&S FSH4 (100 kHz–3.6 GHz) spectrum analyzer. A Tektronix TDS7254B 2.5 GHz–20 GS/s–4 channels oscilloscope has been employed for the time domain measurements.

Figure 4 shows the CM and DM EMI spectra obtained for the two case studies. Both measured spectra show similar low frequency outlines, mainly due to the harmonics of the switching frequency. On the other hand, the induction motor drive has a significant impact on the high frequency EMI profile. Therefore, as expected, the load affects the noise emission profile. In fact, the test bench of case study #1 and #2 is the same, and it differs only for the three-phase load.

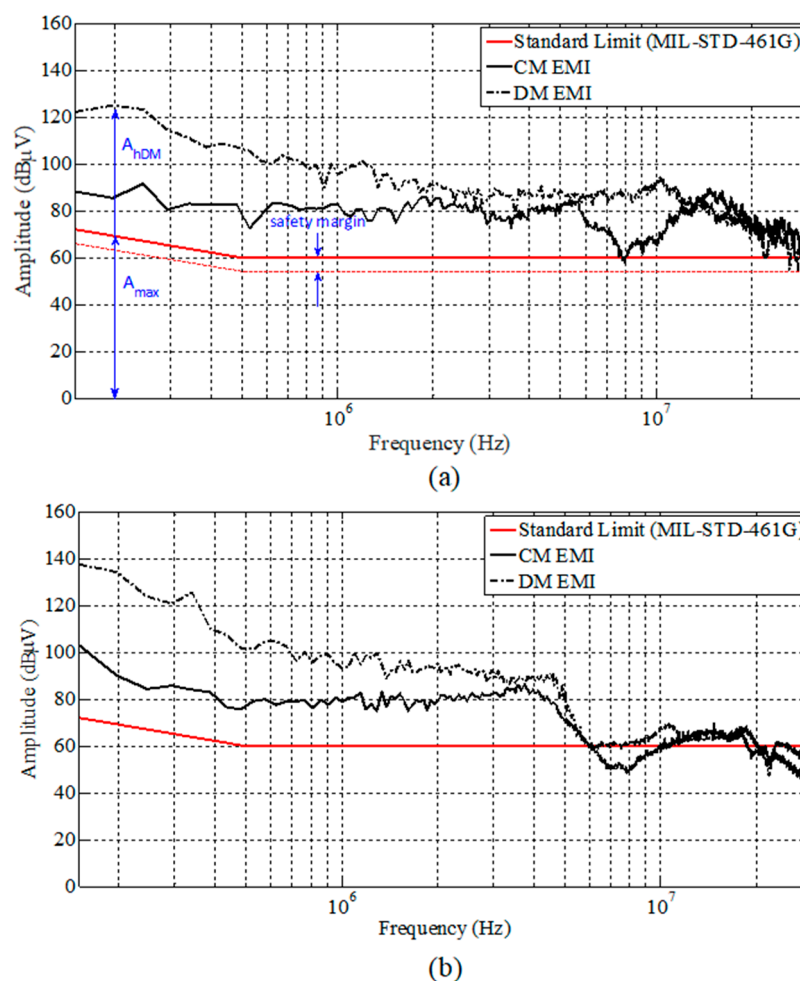


Figure 4. Measured CM and DM EMI for (a) three phase induction motor load (b) three phase resistive load. In (a) the parameters reported in Equations (1) and (2) are also shown.

In both case studies, the limit curve of the Military Standard 461G [28] has been used as the EMI limit standard, a Γ - Π topology for the EMI filter has been considered (Figure 5), the SAE AS 1831 standard has been used for C_y selection, and volume optimization has been selected due to space constraints ($k_{vol} = 100\%$ and $k_{weight} = 0\%$).

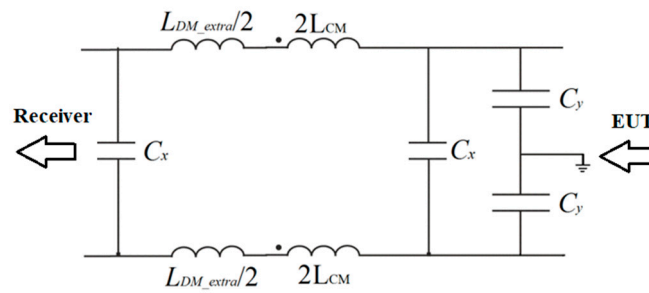


Figure 5. Γ-Π filter topology (single stage) for the experimental setup.

In the first case study, the measured *CM/DM* spectra are used as input data; the following filter parameters have been returned by automatic processing:

- $Att_{CM} = 30 \text{ dB}\mu\text{V}@150 \text{ kHz}$;
- $-Att_{DM} = 60 \text{ dB}\mu\text{V}@170 \text{ kHz}$.

In Table 1, the input data used to run the rule-based algorithm are reported.

Table 1. Input data for the rule-based algorithm—case study #1.

System Type	DC System
V_N	48 V
I_{max_phase}	5 A
I_{cm_max}	32 mA
I_{dm_max}	150 mA
k_{vol}	100%
k_{weight}	0%

In the second case study, the following filter parameters have been obtained by the automatic processing of the measured *CM/DM* spectra:

- $Att_{CM} = 25 \text{ dB}\mu\text{V}@150 \text{ kHz}$;
- $Att_{DM} = 60 \text{ dB}\mu\text{V}@150 \text{ kHz}$.

In Table 2, the input data used to run the rule-based algorithm are reported.

Table 2. Input data for the rule-based algorithm—case study #2.

System Type	DC System
V_N	48 V
I_{max_phase}	150 mA
I_{cm_max}	45 mA
I_{dm_max}	60 mA
k_{vol}	100%
k_{weight}	0%

For case study #1, the best design leads to a double stage ($n_{stages} = 2$) filter without extra *DM* inductors among a total amount of 910 practicable arrangements.

For case study #2, the filter chosen for the experimental validation is one of the 1038 feasible configurations proposed by the design procedure, corresponding to the 28th one. Even if it is not the best configuration in terms of minimum volume, it has been chosen because it is a double stage ($n_{stages} = 2$) filter with an extra L_{DM} : in this way, it is also possible to validate the design procedure in the case of separate *DM* inductors.

Both EMI filters have been set-up. The benchmark is a single stage EMI filter designed and built-up by the conventional procedure [15,29].

To be significant, the filter performance comparison requires the consideration of the same test rig; for this reason, the comparison is performed with the EMI filter designed in [15], highlighting the improvement. The benchmark filter has been designed by using a high permeability nanocrystalline magnetic material for the CM choke. This material has the highest permeability and lowest coercive field strength, ensuring minimal eddy current losses and an outstanding frequency vs. permeability behavior. Furthermore, it is worth noting that the conventional design procedure, in which the cutoff frequency is lower than the power converter switching frequency, determines the same filter in both case studies.

In Tables 3 and 4, the size and performance of the automatically designed filters and the benchmark filter are compared.

Table 3. Filter design output data—case study #1.

	Conventional Design	Automatic Design
Number of Stages	1	2
$L_{CM}@10$ kHz	0.8 mH	126 μ H (each stage)
CM inductor core dimensions (mm \times mm \times mm)	27.9 \times 13.6 \times 12.5	12 \times 8.0 \times 4.5 (each stage)
CM core $A_L@10$ kHz	65.5 μ H (Vitroperm 500F, model T60006-L2025-W380)	28 μ H (Vitroperm 500F, model T60006-L2012-W902) (each stage)
Number of turns per CM winding	5	3 (each stage)
C_{CM}	200 nF	100 nF (each stage)
C_y	100 nF, ceramic, 250 V, (Murata RDER72E104K2)	47 nF, ceramic, 250 V, (Murata RDER72E473K2) (each stage)
$L_{DM}@10$ kHz	1.6 μ H ($L_{leakage} = 0.2\% L_{CM}$)	252 nH ($L_{leakage} = 0.2\% L_{CM}$) (each stage)
C_{DM}	47 μ F, electrolytic, 400 V, (Panasonic EEUEE2G470)	33 μ F, electrolytic, 160 V, (Kemet ESG336M160AH4) (each stage)
Wire size	15 AWG	15 AWG
Volume	25.87 cm ³	13.88 cm ³ (all stages)
Weight	44 g	19.12 g (all stages)

More compact filters are obtained with the automatic procedure, as expected. A reduction of about 56% in weight and about 46% in volume is reached in case study #1; a reduction of about 67% in weight and about 62% in volume is obtained in case study #2.

The automatic processing of the rule-based algorithm allows one to analyze a quite large search space, in order to obtain the arrangement determining the minimum volume/weight: the filter volume ranges from 13.88 cm³ up to 6591 cm³ and from 5.46 cm³ up to 6135.84 cm³ in the worst configuration, respectively, for case study #1 and #2.

The proposed automatic design algorithm stores data related to all feasible configurations. Therefore, it also allows one to perform extra analyses which are not possible with a manual design procedure. In particular, it allows one to compare the best EMI filter design to the suboptimal results: thus, the final choice is left to the designer; moreover, it is possible to evaluate whether an extra safety margin can be obtained whilst maintaining the same optimal value of the objective function.

Table 4. Filter design output data—case study #2.

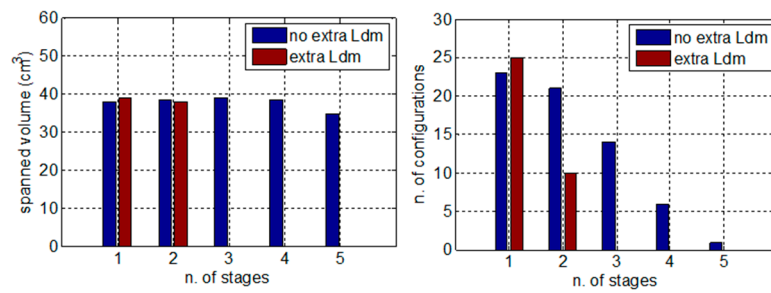
	Conventional Design	Automatic Design
Number of Stages	1	2
$L_{CM}@10$ kHz	0.8 mH	56 μ H (each stage)
CM inductor core dimensions (mm \times mm \times mm)	27.9 \times 13.6 \times 12.5	14.1 \times 6.6 \times 6.3 (each stage)
CM core $A_L@10$ kHz	65.5 μ H (Vitroperm 500F, model T60006-L2025-W380)	28 μ H (Vitroperm 500F, model T60006-L2012-W902) (each stage)
Number of turns per CM winding	5	2 (each stage)
C_{CM}	200 nF	100 nF (each stage)
C_y	100 nF, ceramic, 250 V, (Murata RDER72E104K2)	47 nF, ceramic, 250 V, (Murata RDER72E473K2) (each stage)
$L_{DM}@10$ kHz	1.6 μ H ($L_{leakage} = 0.2\%$ L_{CM})	459 μ H (Extra L_{DM}) (each stage)
DM inductor core dimensions (mm \times mm \times mm)	n.a.	11.2 \times 5.1 \times 5.8 (two for each stage)
DM core $A_L@10$ kHz	n.a.	25.5 μ H (Vitroperm 500F, model T60006-L2009-W914) (2 for each stage)
Number of turns per DM winding	n.a.	3 (each stage)
C_{DM}	47 μ F, electrolytic, 400 V, (Panasonic EEUEE2G470)	33 nF, polypropylene, 560 V, (Kemet 46KF23301P02) (each stage)
Wire size	15 AWG	21 AWG
Volume	25.87 cm ³	9.88 cm ³ (all stages)
Weight	44 g	14.42 g (all stages)

Figure 6 shows the distribution of the 100 best designs around the first best configuration selected by the algorithm. It can be observed that, in the first case study, a relevant number of EMI filter designs are without extra DM inductors. Instead, in the second case study, the low value of the operating current reduces the likelihood of saturation of the magnetic core in the DM section design procedure; therefore, the configurations with extra DM inductors are more numerous, as shown in Figure 6b.

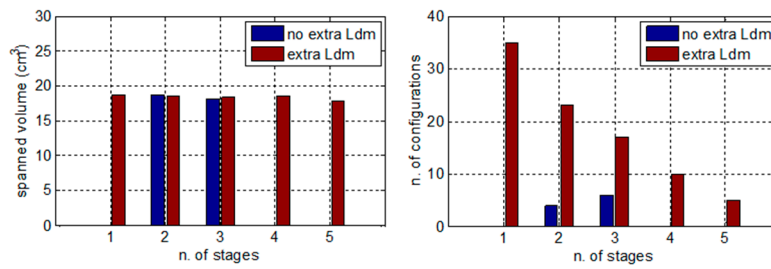
Moreover, the automatic design procedure has been repeated considering fixed input parameters and only increasing the CM attenuation value, starting from the minimum required value. The following range has been swept:

- [30, 32, 34, 36, 38, 40, 42, 44, 46, 48, 50, 52, 54, 56] dB μ V in case study #1;
- [25, 30, 35, 40, 45, 50, 55, 60, 65] dB μ V in case study #2;

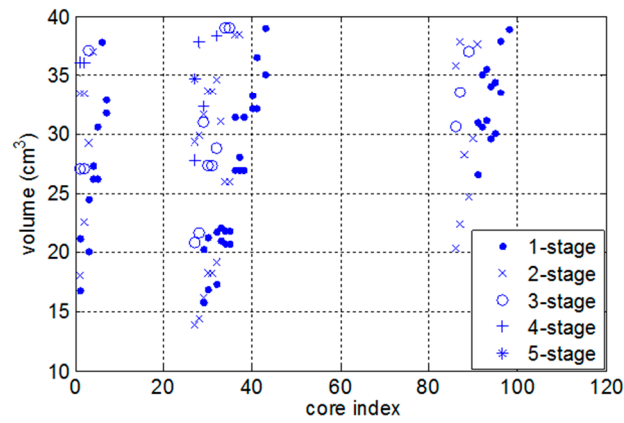
The obtained results for both volume and number of stages are shown in Tables 5 and 6. It can be noted that in both cases, the CM attenuation of the filter can be risen to an extra 10 dB μ V safety margin without increasing the design volume. As a consequence, a better filter performance can be obtained, balancing the unavoidable non-idealities in the filter realization.



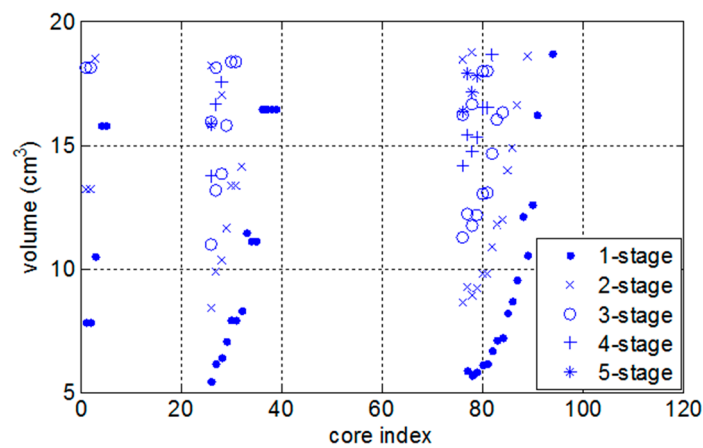
(a)



(b)



(c)



(d)

Figure 6. Scatter plot and distribution of the best 100 configurations in case study #1 (a,c) and in case study #2 (b,d).

Table 5. Volume and number of stages of the best design depending on the required CM attenuation—case study #1.

CM Attenuation (dB μ V)	Number of Stages	Volume (cm ³)
30	2	13.88
32	2	13.88
34	2	13.88
36	2	13.88
38	2	13.88
40	2	13.88
42	1	15.8
44	1	15.8
46	2	16.2
48	2	16.2
50	2	16.2
52	2	18.1
54	2	18.1
56	2	18.3

Table 6. Volume and number of stages of the best design depending on the required CM attenuation—case study #2.

CM Attenuation (dB μ V)	Number of Stages	Volume (cm ³)
25	1	5.46
30	1	5.46
35	1	5.46
40	1	6.19
45	1	6.94
50	1	7.79
55	2	8.43
60	2	8.43
65	2	9.88

In the end, EMI measurements have been carried out in case studies #1 and #2 without any filter, with the conventionally designed filter, and with the automatically designed filter, to assess the filter mitigation performance.

The obtained filters show a good behavior since the filtered EMI meets the limit imposed by the standard under consideration, as shown in Figure 7. Despite the achievement of a higher compactness and power density, the proposed EMI filter design method enables compliance with the reference standard of the power electronic system under consideration, without a significant computational effort.

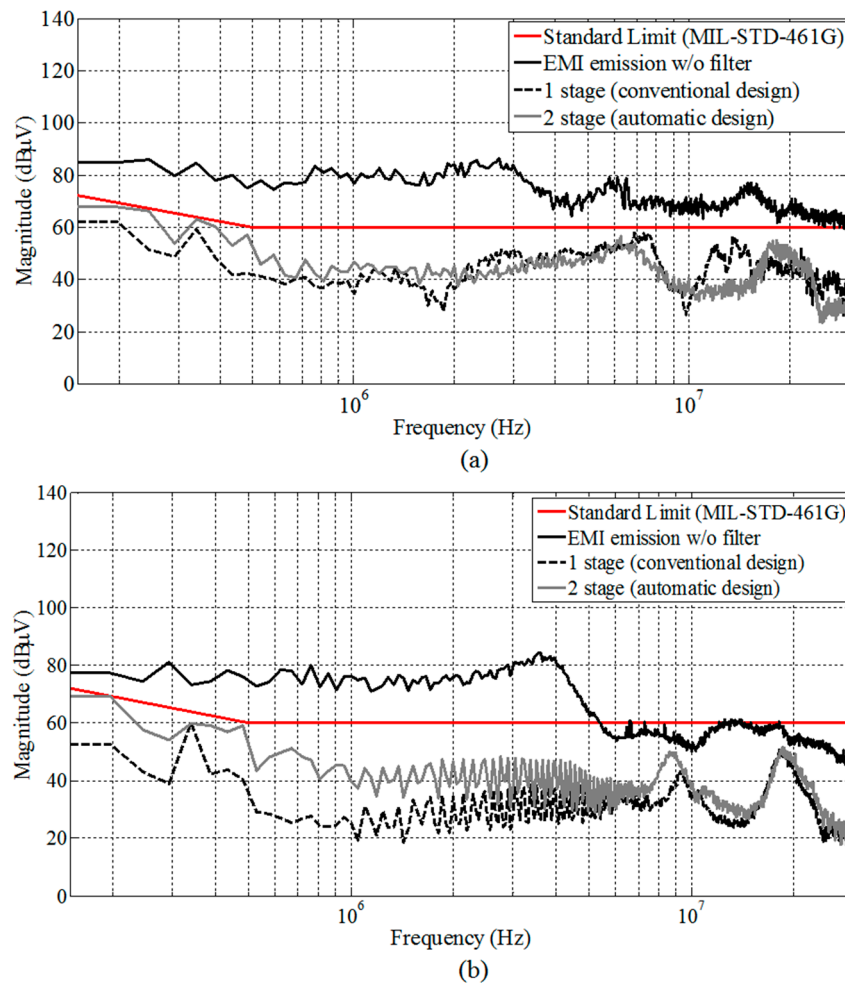


Figure 7. Measured EMI with and without EMI filters (a) case study #1; (b) case study #2.

5. Conclusions

This work proposes an automatic design procedure oriented at obtaining high performing EMI filters with the minimum volume/weight.

The design procedure relies on a suitably devised rule-based algorithm and on databases of magnetic cores, capacitors, and conducting wires suitably selected among those offered by the market. It takes as inputs some relevant parameters that are evaluated from noise measurements and others defining the system arrangement. It outputs the best filter components in terms of performance, volume, and weight. Furthermore, the design procedure allows one to compare the most suitable EMI filter design to the suboptimal results, thus allowing the designer to have a final choice on the configurations to be selected. All the design steps, options, outputs, and design-related additional analyses are handled by the rule-based algorithm without a relevant computational effort. The proposed procedure has been experimentally validated in two case studies, both in terms of performance and increased power density. In addition to the compliance of the power electronic system under study with the reference standard, it has allowed us to achieve EMI filters with a considerable power density and higher compactness if compared with the conventional design.

In particular, an EMI filter size comparison has been carried out, obtaining a reduction of about 56% in weight and about 46% in volume in the first case study, and of about 67% in weight and about 62% in volume in the second case study.

Author Contributions: Guido Ala, Maria Carmela Di Piazza, Graziella Giglia, and Gianpaolo Vitale conceived the research activity; Graziella Giglia and Pericle Zanchetta gave advice on the filter design strategy; Guido Ala, Maria Carmela Di Piazza, and Gianpaolo Vitale conceived the proposed design procedure; Graziella Giglia and Massimiliano Luna performed the software implementation of the rule-based algorithm; Maria Carmela Di Piazza, Massimiliano Luna, Graziella Giglia, and Gianpaolo Vitale devised the test bench; Guido Ala, Giuseppe Costantino Giaconia, and Graziella Giglia contributed to the layout and the measurement set-up; Graziella Giglia performed the filter design and experimental tests; Guido Ala, Maria Carmela Di Piazza, Graziella Giglia, Massimiliano Luna, and Gianpaolo Vitale analyzed the experimental results; Guido Ala, Maria Carmela Di Piazza, and Graziella Giglia wrote the manuscript. All the authors revised and approved the final manuscript.

Conflicts of Interest: The authors declare no conflict of interest.

References

1. Kolar, J.W.; Drofenik, U.; Biela, J.; Heldwein, M.L.; Ertl, H.; Friedli, T.; Round, S.D. PWM Converter Power Density Barriers. In Proceedings of the Power Conversion Conference (PCC '07), Nagoya, Japan, 2–5 April 2007; pp. 9–29.
2. Ahmed, H.F.; Cha, H.; Kim, S.-H.; Kim, D.-H.; Kim, H.-G. Wide Load Range Efficiency Improvement of a High-Power-Density Bidirectional DC–DC Converter Using an MR Fluid-Gap Inductor. *IEEE Trans. Ind. Appl.* **2015**, *51*, 3216–3226. [[CrossRef](#)]
3. Grobler, I.; Gitau, M.N. Modelling and measurement of high-frequency conducted electromagnetic interference in DC–DC converters. *IET Sci. Meas. Technol.* **2017**, *11*, 495–503. [[CrossRef](#)]
4. Grobler, I.; Gitau, M.N. Analysis, modelling and measurement of the effects of aluminum and polymer heatsinks on conducted electromagnetic compatibility in DC–DC converters. *IET Sci. Meas. Technol.* **2017**, *11*, 414–422. [[CrossRef](#)]
5. Hu, B.; Tarateeraseth, V.; See, K.Y.; Zhao, Y. Assessment of electromagnetic interference suppression performance of ferrite core loaded power cord. *IET Sci. Meas. Technol.* **2010**, *4*, 229–236. [[CrossRef](#)]
6. Sun, J.; Chen, W.; Yang, X. EMI Prediction and Filter Design for MHz GaN Based LLC Half-Bridge Converter. In Proceedings of the IEEE 8th International Power Electronics and Motion Control Conference (IPEMC 2016-ECCE Asia), Hefei, China, 22–26 May 2016; pp. 297–304.
7. Kotny, J.L.; Duquesne, T.; Idir, N. Filter design method for GaN-Buck converter taking into account of the common-mode propagation paths. In Proceedings of the IEEE 20th Workshop on Signal and Power Integrity (SPI 2016), Turin, Italy, 8–11 May 2016; pp. 1–4.
8. Liu, Y.; Peng, J.; Wang, G.; Wang, H.; See, K.Y. THD and EMI performance study of foil-wound inductor of LCL filter for high power density converter. In Proceedings of the IEEE 8th International Power Electronics and Motion Control Conference (IPEMC 2016-ECCE Asia), Hefei, China, 22–26 May 2016; pp. 3467–3471.
9. Mallik, A.; Ding, W.; Khaligh, A. A Comprehensive Design Approach to an EMI Filter for a 6-kW Three-Phase Boost Power Factor Correction Rectifier in Avionics Vehicular Systems. *IEEE Trans. Veh. Technol.* **2017**, *66*, 2942–2951. [[CrossRef](#)]
10. Silva, M.; Hensgens, N.; Oliver, J.; Alou, P. New considerations in the input filter design of a three-phase buck-type PWM rectifier for aircraft applications. In Proceedings of the IEEE Energy Conversion Congress and Exposition (ECCE 2011), Phoenix, AZ, USA, 17–22 September 2011; pp. 4087–4092.
11. Danilovic, M.; Luo, F.; Xue, L.; Wang, R.; Mattavelli, P.; Boroyevich, D. Size and weight dependence of the single stage input EMI filter on switching frequency for low voltage bus aircraft applications. In Proceedings of the 15th International Power Electronics and Motion Control Conference (PEMC 2012), Novi Sad, Serbia, 4–6 September 2012; pp. LS4a.41–LS4a.47.
12. Di Piazza, M.C.; Ragusa, A.; Vitale, G. An optimized feedback common mode active filter for vehicular induction motor drives. *IEEE Trans. Power Electron.* **2011**, *26*, 3153–3162. [[CrossRef](#)]
13. Kahoul, R.; Azzouz, Y.; Ravelo, B.; Mazari, B. New Behavioral Modeling of EMI for DC Motors Applied to EMC Characterization. *IEEE Trans. Ind. Electron.* **2013**, *60*, 5482–5496. [[CrossRef](#)]
14. Ala, G.; Di Piazza, M.C.; Giaconia, G.C.; Giglia, G.; Vitale, G. Design and performance evaluation of a high power density EMI filter for PWM inverter-fed induction motor drives. In Proceedings of the IEEE 15th International Conference on Environment and Electrical Engineering (EEEIC 2015), Rome, Italy, 10–13 June 2015; pp. 1573–1579.

15. Ala, G.; Di Piazza, M.C.; Giaconia, G.C.; Giglia, G.; Vitale, G. Design and performance evaluation of a high power density EMI filter for PWM inverter-fed induction motor drives. *IEEE Trans. Ind. Appl.* **2016**, *52*, 2397–2404. [[CrossRef](#)]
16. Maillat, Y.; Lai, R.; Wang, S.; Wang, F.; Burgos, R.; Boroyevich, D. High-Density EMI Filter Design for DC-Fed Motor Drives. *IEEE Trans. Power Electron.* **2010**, *25*, 1163–1172. [[CrossRef](#)]
17. Luo, F.; Dong, D.; Boroyevich, D.; Mattavelli, P.; Wang, S. Improving high-frequency performance of an input common mode EMI filter using an impedance-mismatching filter. *IEEE Trans. Power Electron.* **2014**, *29*, 5111–5115. [[CrossRef](#)]
18. Wang, F.; Shen, W.; Boroyevich, D.; Ragon, S.; Stefanovic, V.; Arpilliere, M. Design Optimization of Industrial Motor Drive Power Stage Using Genetic Algorithms. In Proceedings of the IEEE Industry Applications Conference, Tampa, FL, USA, 8–12 October 2006; pp. 2581–2586.
19. Narayanasamy, B.; Jalanbo, H.; Luo, F. Development of Software to Design Passive Filters for EMI Suppression in SiC DC Fed Motor Drives. In Proceedings of the IEEE 3rd Workshop on Wide Bandgap Power Devices and Applications (WiPDA 2015), Blacksburg, VA, USA, 2–4 November 2015; pp. 230–235.
20. Raggl, K.; Nussbaumer, T.; Kolar, J.W. Guideline for a Simplified Differential-Mode EMI Filter Design. *IEEE Trans. Ind. Electron.* **2010**, *57*, 1031–1040. [[CrossRef](#)]
21. Raggl, K.; Nussbaumer, T.; Kolar, J.W. Model Based Optimization of EMC Input Filters. In Proceedings of the IEEE 11th Workshop on Control and Modeling for Power Electronics (COMPEL 2008), Zurich, Switzerland, 17–20 August 2008; pp. 1–6.
22. Boillat, D.O.; Krismer, F.; Kolar, J.W. EMI Filter Volume Minimization of a Three-Phase, Three-Level T-Type PWM Converter System. *IEEE Trans. Power Electron.* **2017**, *32*, 2473–2480. [[CrossRef](#)]
23. Ala, G.; Di Piazza, M.C.; Giaconia, G.C.; Giglia, G.; Luna, M.; Vitale, G.; Zanchetta, P. Computer Aided Optimal Design of High Power Density EMI Filters. In Proceedings of the IEEE 16th International Conference on Environment and Electrical Engineering (EEEIC 2016), Florence, Italy, 7–10 June 2016; pp. 1–6.
24. Ozenbaugh, R.L.; Pullen, T.M. *EMI Filter Design*, 3rd ed.; CRC Press: Boca Raton, FL, USA, 2011; ISBN 9781439844755.
25. Di Piazza, M.C.; Ragusa, A.; Vitale, G. Common Mode EMI Propagation in High Voltage DC supplied Induction Motor Drives for Electric Vehicles Application. In Proceedings of the IEEE International Electric Machines and Drives Conference (IEMDC 2009), Miami, FL, USA, 3–6 May 2009; pp. 647–652.
26. Anand, S.; Fernandez, B.G. Optimal voltage level for DC microgrids. In Proceedings of the 36th Annual Conference on IEEE Industrial Electronics Society (IECON 2010), Glendale, AZ, USA, 7–10 November 2010; pp. 3034–3039.
27. Kakigano, H.; Nomura, N.; Ise, T. Loss evaluation of DC distribution for residential houses compared with AC system. In Proceedings of the International Power Electronics Conference (IPEC), Sapporo, Japan, 21–24 June 2010; pp. 480–486.
28. Department of Defense. *Military Standard 461G: Requirements for the Control of Electromagnetic Interference Characteristics of Subsystems and Equipment*; AMSC: Devens, MA, USA, 2015.
29. Kumar, M.; Agarwal, V. Power line filter design for conducted electromagnetic interference using time-domain measurements. *IEEE Trans. Electromagn. Compat.* **2006**, *48*, 178–186. [[CrossRef](#)]

